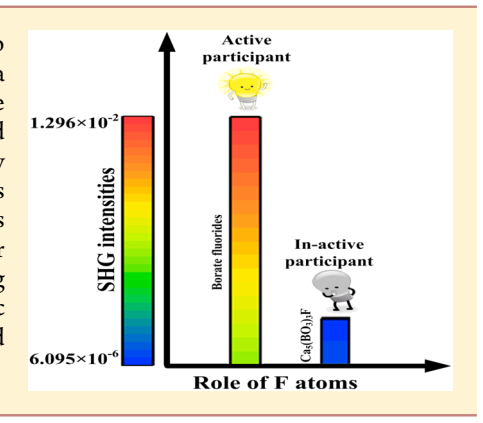


DFT Based Theoretical Study about the Contributions of Fluorine to Nonlinear Optical Properties in Borate Fluoride Crystals

Beenish Bashir, †,‡ Bingbing Zhang, †,‡ Bing-Hua Lei, †,‡ Zhihua Yang, *,† Ming-Hsien Lee, †,§ and Shilie Pan*,†

Supporting Information

ABSTRACT: The introduction of fluorine (F) into the borate crystals is proven to be an effective approach in designing novel non-centrosymmetric crystals, which is a requirement for nonlinear optical (NLO) materials. In this contribution, the electronic structure and optical properties of borate fluoride crystals are determined by the first-principles method. First-principles calculations indicate that the key second-harmonic generation (SHG) factor is attributed not only to borate groups but also to the bonding of the F anions with cations where F coordinates to cations (Sr, Ba). The electron withdrawing effect of the F atom leads to the higher values for anisotropy of the polarizability around cation-centered polyhedra, ultimately making it easy for the external electric field of incident light to effect the dielectric susceptibility. The direct contribution of anion on the NLO properties is observed as fluorine-induced variation of electronic structure.



1. INTRODUCTION

Nonlinear optical (NLO) materials with potential applications in the deep-UV region (i.e., λ < 200 nm) are receiving ever increasing scientific interest. 1-8 Typical characteristics like high value of NLO coefficient, large optical damage threshold, better chemical strength, and possession of short absorption edge of NLO systems make borate crystals a better choice, especially in UV coherent light production. ⁹⁻¹¹ In this regard, many borates have been discovered, like β -BaB₂O₄ (BBO), ¹² LiB₃O₅ (LBO), ¹³ KBe₂BO₃F₂ (KBBF), ¹⁴ and YCa₄O(BO₃)₃ (YCOB), ¹⁵ with potential applications in wide range of spectrum from UV to visible. Recently, some new crystals have been synthesized like Li₄Sr(BO₃)₂, 1 $K_3Ba_3Li_2Al_4B_6O_{20}F$, ¹⁷ MM'Be₂B₂O₆F (where M = Na, M' = Ca; M = K, M' = Ca, Sr), ¹⁸ and Rb₃Al₃B₃O₁₀F. ¹⁹ Thus, borates have attracted intense attention regarding the development of novel UV NLO crystals. 20-27 Currently, it is still desirable and challenging to synthesize useful NLO materials with large NLO response, possessing a wide window in the UV region to offer real-world applications and lying in the deep UV-region in particular. 28-31 So it is very important to get deep understanding about the association between the composition of elements, type of crystal configuration, and NLO characteristics of materials. According to the anionic group theory,³² established by Chen,³³ the total nonlinearity exhibited by the crystal is a geometric superposition of the microscopic second order susceptibility tensors of the NLO-active anionic groups.

Furthermore, the concept that the anionic groups are major contributors to generating the NLO effect was also verified successfully during the development of various novel NLO materials in the borate systems.34

Along with anionic groups, we have also introduced elements from group 1A and 2A metals and group 7A elements, that is, fluorine (F) atoms, in a unique deep UV crystal for the following reasons. First, group 1A or 2A metal cations are helpful in transmitting UV light due to the absence of d-d or f-f electronic transitions in this region of the spectrum and the negative impact of closed orbital d or f electronic transitions on the energy band. 17,35-38 Thus, 1A and 2A metal borates are potential systems to design and develop for new innovative NLO materials, also proving themselves worthy of future research. Second, the introduction of halogens into borate systems has attracted much attention from researchers for the development of new NLO borates, exhibiting eye-catching characteristics. The strong electronegativity of halogen (fluorine) results in a large band gap, ensuring short UV cutoff edge in the crystal and blue shift in the absorption spectrum,³⁸ where a strong attribution to this property is studied and described in crystals like $KBe_2BO_3F_2$, 39 ABCO₃F (where A = K, Rb, Cs; B = Ca, Sr, Ba), 40 and NaSr₃Be₃B₃O₉F₄. 41

Received: May 2, 2016 Revised: August 8, 2016 Published: August 9, 2016

[†]Key Laboratory of Functional Materials and Devices for Special Environments, Xinjiang Technical Institute of Physics & Chemistry, Chinese Academy of Sciences, Xinjiang Key Laboratory of Electronic Information Materials and Devices, 40-1 South Beijing Road, Urumqi 830011, China

[‡]University of Chinese Academy of Sciences, Beijing 100049, China

[§]Department of Physics, Tamkang University, New Taipei City 25137, Taiwan

Advanced scientific computational resources based on first-principles calculations are helpful to analyze the connection between the behavior of electronic structure and ultimately the optical response of the materials. Also, NLO properties based on electronic structure can be further analyzed depending upon the exploration of electronic structure of the crystals. Thus, band-resolved⁴² and SHG-density⁴³ methods are better suited for the estimation of the dominant contribution of orbitals and atoms or group of atoms to enhance the SHG response. These findings can be intensively beneficial for the deep understanding of the basic mechanism of NLO response, playing a leading role for the development of new NLO materials.

Fabianite-like borate halides, for example, $Sr_3B_6O_{11}F_2^{44}$ and $Ba_3B_6O_{11}F_2^{38,44}$ show low UV cutoff edge (i.e., less than 190 nm) with their unique system making them extremely favorable for deep-UV NLO applications. The powder SHG (PSHG) intensity of Sr₃B₆O₁₁F₂ and Ba₃B₆O₁₁F₂ are 2.5× and 3×, respectively, that of potassium dihydrogen phosphate (KDP). 45,38 They crystallize in monoclinic space group P21, having unique fundamental building units (FBU) and distorted cation centered polyhedra, and relate the crystal structure at microscopic level and NLO response at macroscopic level, providing valuable research matter to seek better understanding among the preceding quantities. In response to large electronegativities of halogens, the introduction of the F in borate crystals is beneficial for the transparency in the UV-region, for example, KBe₂BO₃F (KBBF). The introduction of the F in Ba₄B₁₁O₂₀F⁴⁶ compound shifts the UV absorption edge into the deep-ultraviolet (DUV) region, approximately at 175 nm. Also, Ba₄B₁₁O₂₀F has unique fundamental building units [FBU] and distorted cation centered polyhedra where F atoms are connected to the cations only, like Sr₃B₆O₁₁F₂ and Ba₃B₆O₁₁F₂

So, to determine the influence of F on structure, electronic structure, and optical properties in alkaline earth metal borates, Sr₃B₆O₁₁F₂ is investigated as representative. Also, electronic structure comparison of Sr₃B₆O₁₁F₂ with Sr₄B₁₀O₁₈(OH)₂· 2H₂O⁴⁷ helps us in understanding the role of F in NLO materials. In order to develop an understanding regarding the effect of F, the first-principles methods are employed to explore the electronic and NLO properties of Sr₃B₆O₁₁F₂. To resolve the curiosity about the origins of SHG response and to learn about role of F as NLO-active component in borate fluorides, the following strategy was adopted: band-resolved method and SHG density method have been implemented to understand affiliation between electronic structure and NLO properties. Detailed analysis reveals that borate groups are not the only players in generating the basic SHG factor; instead it is the bonding of the F anions in borate fluoride crystals that also contributes in the generation of the SHG response. It is estimated that introducing the F atoms into borate crystals can make the structures and properties more diverse in nature due to its larger electronegativity compared with the O anions.

2. COMPUTATIONAL METHODOLOGY

In order to examine the electro-optical properties of studied crystals, CASTEP, ^{48,49} a plane wave pseudo-potential method on the basis of density functional theory (DFT), was employed. Numbers of successful calculations were performed, while in the end, the exchange correlation functional Perdew–Burke–Ernzerhof (PBE) has been employed under the limits of the generalized gradient approximation (GGA).⁵⁰ Norm conserving pseudopotential (NCP)^{49–53} was employed as the pseudopotential, and the valence electron configuration was fixed as Sr 4s²4p⁶5s², Ca 3s²3p⁶4s², Ba 5s²5p⁶6s²,

$$\chi_{\alpha\beta\gamma}^{(2)} = \chi_{\alpha\beta\gamma}^{(2)}(VE) + \chi_{\alpha\beta\gamma}^{(2)}(VH) + \chi_{\alpha\beta\gamma}^{(2)}(two bands)$$
 (1)

In the preceding two states summation formalism, the whole SHG coefficient, $\chi^{(2)}_{\alpha\beta\gamma}$ is shared among the individual contributions of processes like virtual electron (VE), virtual hole (VH), and two band (TB), but the TB process has exactly zero contribution, ⁵⁶ while the formulation for calculating $\chi^{(2)}_{\alpha\beta\gamma}(VE)$ and $\chi^{(2)}_{\alpha\beta\gamma}(VH)$ are as follows:

$$\chi_{\alpha\beta\gamma}^{(2)}(VE) = \frac{e^3}{2\hbar^2 m^3} \sum_{vv'c} \int \frac{d^3k}{4\pi^3} P(\alpha\beta\gamma) Im[P_{vv}^{\alpha} P_{cv}^{\beta} P_{cv}^{\gamma}]$$

$$\left(\frac{1}{\omega_{cv}^3 \omega_{v'c}^2} + \frac{2}{\omega_{v'}^4 \omega_{cv'}}\right)$$
(2)

$$\chi_{\alpha\beta\gamma}^{(2)}(VH) = \frac{e^3}{2\hbar^2 m^3} \sum_{\nu cc'} \int \frac{d^3k}{4\pi^3} P(\alpha\beta\gamma) \operatorname{Im}[P_{c\nu}^{\alpha} P_{cc'}^{\beta} P_{c'\nu}^{\gamma}]$$

$$\left(\frac{1}{\omega_{c\nu}^3 \omega_{\nu c'}^2} + \frac{2}{\omega_{\nu c}^4 \omega_{c'\nu}}\right)$$
(3)

where α , β , and γ are Cartesian constituents, ν and ν' are notations for valence bands, c and c' belong to conduction bands, and $P(\alpha\beta\gamma)$ symbolizes full permutation, whereas $\hbar\omega_{ij}$ is donated to band energy difference and P_{ij}^a shows momentum matrix components.

The effective contribution of each electronic state to SHG susceptibilities can be represented as occupied and unoccupied bands that clearly describe the orbital contribution to total $\chi^{(2)}$. Thus, integral SHG coefficient can be shown in energy regions that identify and analyze the contribution of dominant orbitals to total $\chi^{(2)}$. Thus, to identify and analyze the main contribution of dominant orbitals to the SHG process, the band-resolved method was employed. Detailed description of this method has been published already. Furthermore, SHG density method was also employed to confirm the dominant contribution of electronic structure of subunits that enhance the SHG response. The resulting distribution of density developed by occupied states or unoccupied states is very useful in highlighting the origin of SHG optical nonlinearity. The preceding methods have already proven their worth in order to categorize the origin of SHG in different borate materials as investigated in refs 56 and 58.

3. RESULTS AND DISCUSSION

3.1. Crystal Structure Description. Borate fluorides like $Sr_3B_6O_{11}F_2$, $Ba_3B_6O_{11}F_2$, and $Ba_4B_{11}O_{20}F$, have a complicated structure framework, which consists of a 3D B–O network, created by different FBUs with tunnels, where metal and fluorine atoms are located. Thus, it is concluded that the gaps present in the borate framework are fulfilled by the cation centered polyhedra generating their own particular network. Because $Sr_3B_6O_{11}F_2$ and $Ba_3B_6O_{11}F_2$ are isostructural, they show the similar structural features, while $Ba_4B_{11}O_{20}F$ belongs to polar space group $Cmc2_1$.

Crystal structure details for $Sr_3B_6O_{11}F_2$ are listed in Table S1 in the SI. $Sr_3B_6O_{11}F_2$ crystallizes in noncentrosymmetric (NCS) chiral and polar group $P2_1$. Figure 1a exhibits that $[B_6O_{14}]$ FBUs and cation centered polyhedra (SrO_nF_2 , n=7, 8) form an anionic 3D network in order to manufacture the

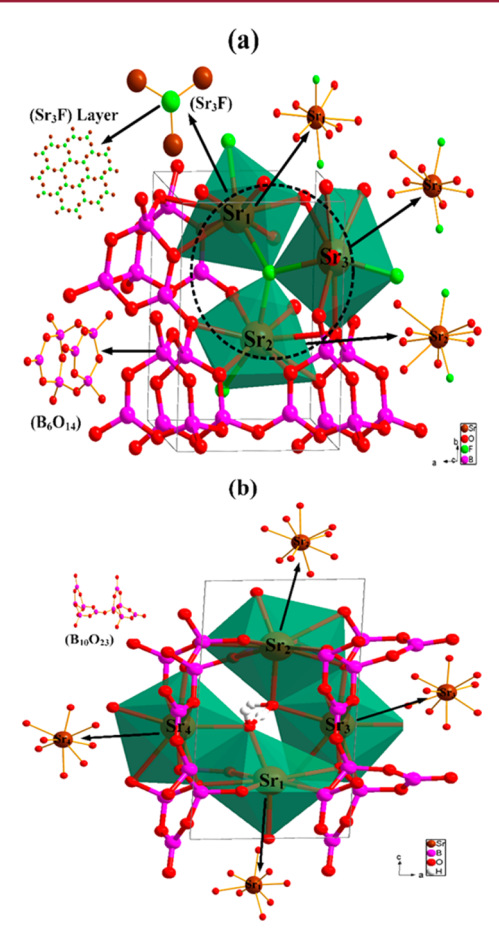


Figure 1. Three-dimensional framework of (a) $Sr_3B_6O_{11}F_2$ and (b) $Sr_4B_{10}O_{18}(OH)_2\cdot 2H_2O$ crystal with arrangements of Sr containing polyhedra in respective crystals. In $Sr_3B_6O_{11}F_2$, the [FSr₃] units connect with each other to form 2D [F_2M_3] layers.

complex crystal structure of Sr₃B₆O₁₁F₂. Four BO₄ tetrahedra are attached with two BO3 triangles to form [B6O14] as the FBU. When observed in the direction of the b-axis (Figure 1), the Sr cation and F anion form layers, where [101] is the direction of extension of the [FSr₃] layer. Following a similar pattern to Cd₅(BO₃)₃F⁵⁹ and Ca₅(BO₃)₃F⁶⁰ structures, there is a direct bond between the F anions and the cation (Sr) atoms only instead of B atoms in Sr₃B₆O₁₁F₂. Thus, the FBU (borate oxide) and [FSr₃] layers act like organic-inorganic hybrid systems that show host-guest behavior among them. 61 These layers form a 3D network interconnected to the borate fundamental building block covalent framework through oxygen (O) bridging atoms. Thus, Sr containing polyhedra reside in the gaps of the framework of the borate. So Sr-F planes cause the parallel arrangement of the BO3 groups between the Sr-F planes, as partial replacement of the O atoms by the F atoms affects the surrounding environment of the Sr atoms. Thus, Sr-F layers have an impact on the distribution of polymerization of the anionic structure in the compound.

Crystal data for $Ba_4B_{11}O_{20}F$ are listed in Table S1 in the SI. The crystal structure of $Ba_4B_{11}O_{20}F$ (Figure S1 in the SI) like $Sr_3B_6O_{11}F_2$ consists of two parts, $[B_{11}O_{24}]$ FBUs and distorted cation centered polyhedra. Five $[B_3O_8]$ rings are connected through oxygen atoms and create a 3D network with tunnels extending along the *c*-axis. In the FBU, B atoms have BO_3 triangles and BO_4 tetrahedra coordination environments. The F anions in $Ba_4B_{11}O_{20}F$ system are just connected to Ba atoms

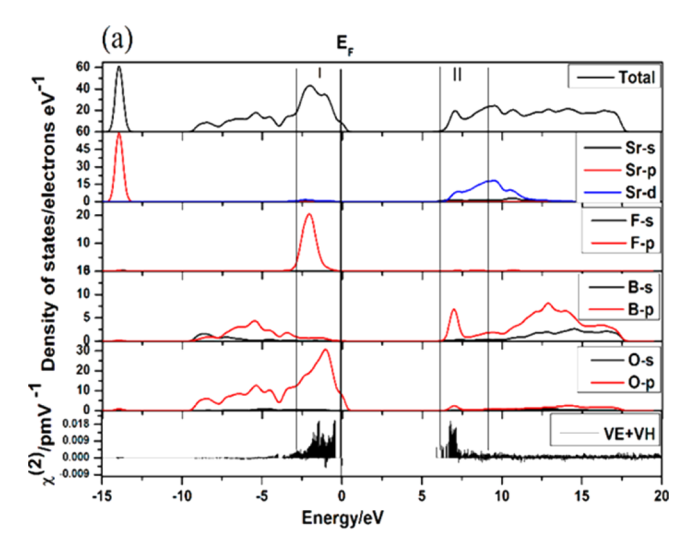
instead of being part of the FBU like $Sr_3B_6O_{11}F_2$. The Ba cation and F anion form [FBa₃] groups in chains, which fill in the tunnels formed by the BO network. Thus, Ba containing polyhedra form their own network and reside in the gaps of the framework of borate like in $Sr_3B_6O_{11}F_2$.

As a comparison, the structure $Sr_4B_{10}O_{18}(OH)_2 \cdot 2H_2O$, without the F atom, is described. Crystal data for $Sr_4B_{10}O_{18}(OH)_2 \cdot 2H_2O$ are listed in Table S1 in the SI, having symmetry of polar space group P1. As shown in Figure 1b, the structure of $Sr_4B_{10}O_{18}(OH)_2 \cdot 2H_2O$ has $B_{10}O_{23}$ groups as FBUs, which are comprised of four BO_3 and six BO_4 units. The hydroxyl group and H_2O molecule are connected to the cation (Sr) only, instead of being part of the FBU in the crystal. Thus, the gaps in the network of the FBUs are filled by the network of Sr atom polyhedra.

The electron withdrawing ability of F leads to the higher local polarization of Sr containing polyhedral in Sr₃B₆O₁₁F₂ compared with Sr polyhedra without F in Sr₄B₁₀O₁₈(OH)₂· 2H₂O compound, which leads to the total SHG response. Compared with the other crystals, like $Sr_3B_6O_{11}(OH)_2^{62}$ and $Sr_4B_{10}O_{18}(OH)_2 \cdot 2H_2O_1$, the SrO_nF_2 (n = 7, 8) polyhedral in Sr₃B₆O₁₁F₂ show remarkable distortions due to substitution of O by F, like angle reduction for O-Sr-O (46° and 168°) in Sr₃B₆O₁₁F₂ with respect to O-Sr-O (51° and 174°) in $Sr_3B_6O_{11}(OH)_2$ and O-Sr-O (51° and 174°) in Sr₄B₁₀O₁₈(OH)₂·2H₂O₂, along with longer Sr-O distance $(2.49-3.20 \text{ Å}) \text{ vs } Sr_3B_6O_{11}(OH)_2 (2.42-2.88 \text{ Å}) \text{ and}$ $Sr_4B_{10}O_{18}(OH)_2 \cdot 2H_2O$ (2.49-2.96 Å). These preceding structural factors, that is, bond lengths and bond angles, exhibit a significantly increasing distortion in SrO_nF_2 (n = 7, 8) polyhedral in Sr₃B₆O₁₁F₂, which originates from the introduction of more electronegative F anions. Thus, owing to its larger electronegativity compared with O anions, the introduction of F anions into the borate crystals can cause more diversity in their structures and properties.

3.2. Electronic Structure and Properties. Owing to the direct relation of energy band gap to the optical properties of crystal, wide band gap is a basic requirement in UV NLO materials that leads to a short UV absorption edge. ^{14,63} Thus, it has proved to be a challenging task to formulate and synthesize short absorption edge NLO materials that particularly exist in the deep UV region due to the involvement of subtle variations in the relationships among properties, structure, and composition. ⁶⁴

The calculated band structure for crystals Sr₃B₆O₁₁F₂, $Ba_3B_6O_{11}F_2$, and $Sr_4B_{10}O_{18}(OH)_2 \cdot 2H_2O$ are exhibited in the directions of high symmetry in the Brillouin zone (BZ) in Figure S2 in the SI. Because $Sr_3B_6O_{11}F_2$ is isostructural to Ba₃B₆O₁₁F₂, their electronic structures are qualitatively similar to each other as described in Figure 2 and Figure S2 in the SI. Here only the electronic structure of $Sr_3B_6O_{11}F_2$ is explained in detail as a representive of fabianite-like borate fluorides. The electronic structures of title compounds, calculated from GGA, reveal that Sr₃B₆O₁₁F₂ and Sr₄B₁₀O₁₈(OH)₂·2H₂O are direct band gap insulators having underestimated band gaps of 5.66 and 5.32 eV, respectively, where calculated band gap is smaller than experimental results owing to the discontinuity associated with GGA.⁶⁵⁻⁶⁷ However, to get linear or nonlinear optical properties accurately, which depend upon the DFT band structure calculations, the scissors operator 68-70 was used. The scissors operator can be defined as the difference of the experimental band gap from the calculated band gap value. Thus, scissors approximation is used for gap correction by



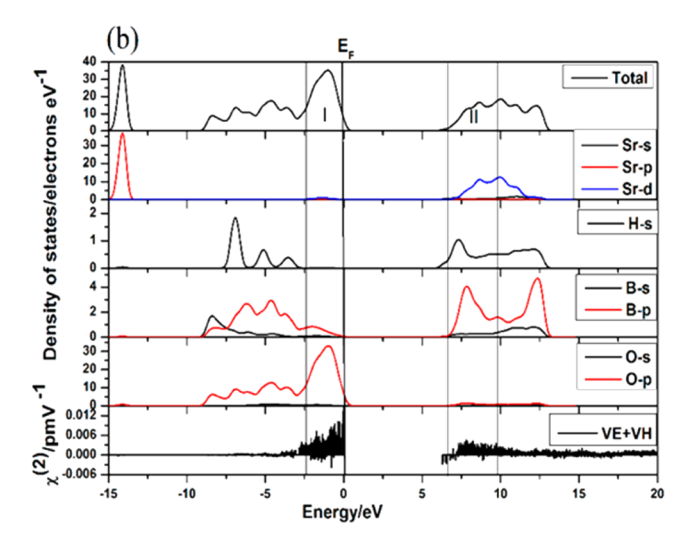


Figure 2. PDOS (top) and band-resolved $\chi^{(2)}$ (bottom) of (a) $\mathrm{Sr_3B_6O_{11}F_2}$ and (b) $\mathrm{Sr_4B_{10}O_{18}(OH)_2\cdot 2H_2O}$. The PDOS and band-resolved $\chi^{(2)}$ demonstrate the significant contributions to the SHG effect from region I of VBs and region II of CBs.

shifting all the conduction bands away from the valence bands. Moreover, other types of pseudopotentials are also used for the calculation of bands. However, no significant change in the results is observed [Table S2 in the SI]. Because the states close to the band gap are of vital importance for the determination of the optical properties of a crystal in the visible and UV spectra,³⁴ we present a careful analysis of the regions close to the band gap, that is, the top and bottom of the valence and conduction bands, respectively. In order to get valuable information about composition and enrollment of orbitals and type of bonding, the partial density of states (PDOS) is an important tool. The information is composed along with the PDOS of $Sr_3B_6O_{11}F_2$, and their participation in $\chi^{(2)}$ obtained by the band-resolved method is also plotted, in comparison with those of Sr₄B₁₀O₁₈(OH)₂·2H₂O shown in Figure 2b. Depending upon the deviation in the band-resolved $\chi^{(2)}$, the PDOS is divided into several regions of energy. Figure 2 of the PDOS shows the dominance of O 2p states from -9.5 eV to near Fermi level for Sr₃B₆O₁₁F₂, whereas the O 2p of Sr₄B₁₀O₁₈(OH)₂·2H₂O shows its dominance below Fermi level from -8.6 to -2.5 eV. It defines an obvious hybridization

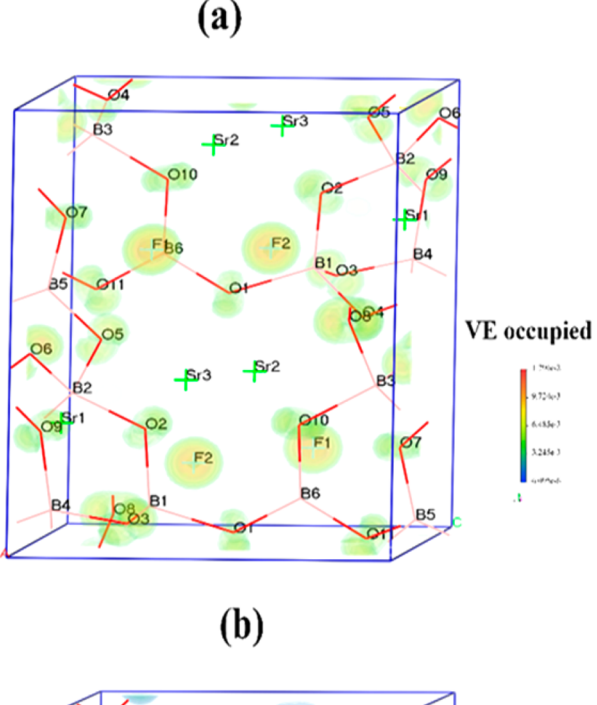
among the 2p states of boron (B) and oxygen (O) atoms in the region of valence band extending from -8 to -3 eV for $Sr_3B_6O_{11}F_2$ and from -7.5 to -2.5 eV for $Sr_4B_{10}O_{18}(OH)_2 \cdot 2H_2O$, respectively.

States from F are mainly predominant between -3.3 and -0.5 eV. There is a localization of the orbitals of cations of both the compounds in the deep region of the VB, thus having a minute chance of mixing with their other neighboring atoms. Usually, 2p states from B and O atoms and the orbitals of Sr determine the bottom of CBs in both compounds. The states of Sr mainly occupy the region above E_F , implying that the role of Sr is electron donor, and F anions occupy the region below $E_{\rm F}$, implying the role of F anions is electron acceptor, in $Sr_3B_6O_{11}F_2$. Additionally, in the case of $Sr_4B_{10}O_{18}(OH)_2$. 2H₂O, resulting from the formation of the O-H groups, there occurs hybridization among the H 1s orbitals and O atoms electronic states; however it has no significant contribution toward VB and CB. Usually, there is a strong relationship among the optical properties and electronic transitions occurring near $E_{\rm F}$ to the bottom of the CB from the top of the VB. Thus, we come to evidence that the band gap is mainly determined by the interactions between BO groups in both crystals but contributions of the F anions in Sr₃B₆O₁₁F₂ cannot be ignored. The presence of occupied 2p states of F atoms with occupied 2p states of O atoms near $E_{\rm F}$ decrease the energy of VB leading to larger band gap, attributed to larger electronegativity of F atoms compared with O atoms. Ultimately, when exposed to incident light for electronic excitation, the F atoms need more energy. Thus, the introduction of F atoms in borates could participate in shifting the absorption edge to the UV or deep UV region.

Similar results are also obtained from electronic band structures of $Ba_3B_6O_{11}F_2$ and $Ba_4B_{11}O_{20}F$ (Figure S3 in the SI). We considered the contribution of F anions in another crystal, $Ca_5(BO_3)_3F$, where F is only coordinated to Ca cations and is not directly a part of borate lattices. As described by the PDOS of $Ca_5(BO_3)_3F$ in Figure S4 in the SI, the BO_3 anionic groups exhibit a governing contribution for the generation of SHG effect, but F anions have no direct contribution like in above studied crystals. The F atom is not located near the Fermi level, and the states from F atoms mainly extend between -5 and -3 eV in the VB.

So we can deduce that in $\mathrm{Sr_3B_6O_{11}F_2}$ crystal, the F undergoes asymmetric electron distribution in Sr centered polyhedra, because F is more electronegative than O, leading to higher local polarization, since p orbitals of F atoms near the E_{F} have a direct effect on the NLO properties of crystal. These results are further confirmed by SHG density calculations. Figure S5 in the SI describes the shapes of orbitals regarding the regions of interest that confirm the orbital calculation results.

3.3. Optical Properties. The SHG coefficients of the considered systems calculated theoretically are presented in Table S3 in the SI and are compared with their corresponding experimental values. ^{38,48,60} The theoretically calculated SHG coefficients, using first-principles method, and the experimental results are in fair agreement for the studied crystal, thus verifying the level of accuracy and application validity of the first principle methods. To determine the role of anions toward the second order susceptibility, a SHG density method is employed, which defines the total contributions from VE and VH processes; however, in the present work the VE process, which makes the occupied state, is examined owing to its dominance toward the SHG effect. Figure 3a gives a clear



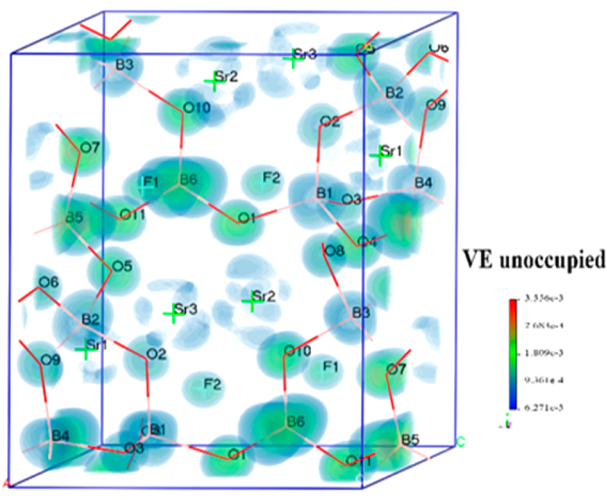


Figure 3. SHG density of (a) occupied states and (b) unoccupied states of $Sr_3B_6O_{11}F_2$ in the VE process.

description that SHG densities on O atoms are dominant along with the F atoms in Sr₃B₆O₁₁F₂. From the unoccupied states, Figure 3b shows that SHG densities are mainly accumulated on B and O atoms (B5O₃, B6O₃), in addition to the O atoms in the BO₄ tetrahedron, all showing large SHG densities, which proves a significant role of B-O groups. It is remarkably interesting to note that all F atoms exhibit large SHG densities. Similarly, depending upon the non-negligible SHG densities around Sr cations, its contribution also cannot be ignored. The same behavior has been observed in Ba₄B₁₁O₂₀F as shown in Figure S6 in the SI. However, the SHG density of occupied states exhibit its dominance on the F atoms, thus verifying its importance for SHG generation. We also calculated SHG density for Ca₅(BO₃)₃F and compared the results with those of Sr₃B₆O₁₁F₂ and Ba₄B₁₁O₂₀F. Figure S7 of the SI is a description of the accumulation of the SHG density of Ca₅(BO₃)₃F on the B and O atoms only, thus providing substantial evidence of the generation of SHG coefficient by the BO3 anionic groups; however the F atoms contribution is negligible. It has been

discussed that the position of the F is away from the Fermi level in $\text{Ca}_5(\text{BO}_3)_3\text{F}$ and the F has different coordination environment compared with other studied borate halides.

A comparison between the PDOS of F atoms of $Sr_3B_6O_{11}F_2$, $Ba_3B_6O_{11}F_2$, $Ba_4B_{11}O_{20}F$, and $Ca_5(BO_3)_3F$ compounds with the integral of band-resolved $\chi^{(2)}$ is shown in Figure 4. The result

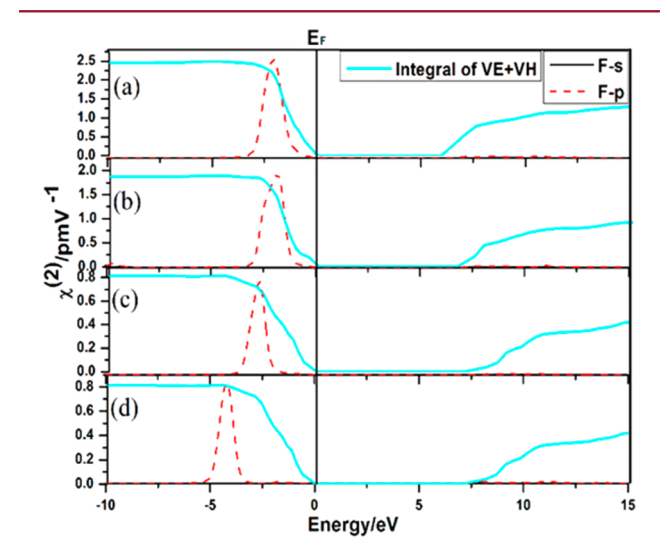


Figure 4. Comparison of the partial density of states (PDOS) of F atoms and integral of VE + VH (cyan line) for (a) $Sr_3B_6O_{11}F_2$, (b) $Ba_3B_6O_{11}F_2$, (c) $Ba_4B_{11}O_{20}F$, and (d) $Ca_5(BO_3)_3F$ compounds.

illustrates that the F atoms in $Sr_3B_6O_{11}F_2$, $Ba_3B_6O_{11}F_2$, and $Ba_4B_{11}O_{20}F$ have a direct contribution to the SHG response as the gradient of the integral of band-resolved $\chi^{(2)}$ increases. As mentioned earlier, the F atoms in crystals led to a large degree of distortion to cation centered polyhedra and stimulated the discrepancy of electronic structures. The direct contribution of the F atoms can cause the absorption edge to blue shift toward the UV or deep UV region (λ < 200 nm).

In the case of $Ca_5(BO_3)_3F$, according to unchanged feature of integral of band-resolved $\chi^{(2)}$, the F atoms have much smaller direct contribution to SHG response because the 2p states of F atoms are not located near the E_F .

Based on PDOS and SHG density analysis, it is concluded that the B–O groups have a dominant role in SHG response. The F atoms serve as NLO-active participants in the studied borate fluoride crystals.

4. CONCLUSIONS

In order to develop an understanding of the effect of F, first-principles methods are employed to examine the electronic and NLO properties of borate fluorides. Detailed analysis reveals that the key SHG factors are attributed not only to borate groups but also to the F anions in borate fluorides. Introduction of the F, due to more electronegativity than the O atoms, led to large degree of distortion in structural units of the studied borate fluoride crystals. Importantly, the highly distorted cation polyhedra is due to presence of F atoms with significant influence on the NLO properties rather than affecting the structures of the studied crystal systems. The F atoms serve as a NLO-active participant in the studied borate fluoride crystals. The direct effect of the F atoms on the NLO properties is observed as the F atoms stimulate the variation of electronic structures in studied borate fluoride crystals.

Our comprehensive analysis on borate fluorides shows the functionality of the F atoms in crystal structure, which may reveal generally instructive and broader possible effects on the discovery of new NLO materials in the future. In materials, the presence of the F atoms with larger electronegativity than the O atoms could cause absorption edge to blue shift toward the UV/DUV region. Also, future work will seek to elaborate this study to explore new materials, which will open a new window and serve as pioneer for the researchers to theoretically predict, experimentally synthesize, and develop innovative UV/DUV, new generation fluorine-containing crystals depending upon the role of F, as investigated in the present study, that will fulfill the demands in laser technologies.

ASSOCIATED CONTENT

S Supporting Information

The Supporting Information is available free of charge on the ACS Publications website at DOI: 10.1021/acs.cgd.6b00662.

Crystal descriptions of $Sr_3B_6O_{11}F_2$, $Ba_3B_6O_{11}F_2$, $Ba_4B_{11}O_{20}F$, and $Sr_4B_{10}O_{18}(OH)_2\cdot 2H_2O$, calculated band gaps of studied compounds, calculated SHG coefficients with experimental values for $Sr_3B_6O_{11}F_2$, $Ca_5(BO_3)_3F$, and $Sr_4B_{10}O_{18}(OH)_2\cdot 2H_2O$, 3D framework of $Ba_4B_{11}O_{20}F$ and $Ba_3B_6O_{11}F_2$, band structures of $Sr_3B_6O_{11}F_2$, $Ba_3B_6O_{11}F_2$, $Ba_4B_{11}O_{20}F$, $Ca_5(BO_3)_3F$, and $Sr_4B_{10}O_{18}(OH)_2\cdot 2H_2O$, PDOS with band-resolved $\chi^{(2)}$ of $Ba_3B_6O_{11}F_2$ and $Ba_4B_{11}O_{20}F$, PDOS with band-resolved $\chi^{(2)}$ of $Ca_5(BO_3)_3F$, some respective orbitals of $Sr_3B_6O_{11}F_2$, and SHG densities of $Ba_4B_{11}O_{20}F$ and $Ca_5(BO_3)_3F$ in the VE process (PDF)

AUTHOR INFORMATION

Corresponding Authors

*E-mail: zhyang@ms.xjb.ac.cn (Zhihua Yang).

*E-mail: slpan@ms.xjb.ac.cn (Shilie Pan). Tel (+86)991-3810816. Fax: (+86)991-3838957.

Notes

The authors declare no competing financial interest.

ACKNOWLEDGMENTS

This work is supported by National Basic Research Program of China (Grant No. 2014CB648400), the National Natural Science Foundation of China (Grant Nos. 11474353 and 51425206), the Recruitment Program of Global Experts (1000 Talent Plan, Xinjiang Special Program), the Instrument Developing Project of the Chinese Academy of Sciences (Grant No. YZ201349), Xinjiang Program of Introducing High-Level Talents. Authors are also delighted to extend special thanks to CAS—TWAS president fellowship for academic and financial facilitation.

REFERENCES

- (1) Kong, F.; Huang, S. P.; Sun, Z. M.; Mao, J. G.; Cheng, W. D. J. Am. Chem. Soc. **2006**, 128, 7750–7751.
- (2) Zhang, W. L.; Cheng, W. D.; Zhang, H.; Geng, L.; Lin, C. S.; He, Z. Z. J. Am. Chem. Soc. **2010**, 132, 1508–1509.
- (3) Maggard, P. A.; Stern, C. L.; Poeppelmeier, K. R. J. Am. Chem. Soc. 2001, 123, 7742–7743.
- (4) Gao, J.; Song, L.; Hu, X.; Zhang, D. Solid State Sci. 2011, 13, 115-119.
- (5) Ikonnikov, D. A.; Malakhovskii, A. V.; Sukhachev, A. L.; Zaitsev, A. I.; Aleksandrovsky, A. S.; Jubera, V. Opt. Mater. 2012, 34, 1839—1842.

(6) Xu, X.; Hu, C.-L.; Kong, F.; Zhang, J.-H.; Mao, J.-G.; Sun, J. Inorg. Chem. **2013**, 52, 5831–5837.

- (7) Reshak, A. H.; Auluck, S.; Kityk, I. V. Phys. Rev. B: Condens. Matter Mater. Phys. 2007, 75, 245120.
- (8) Wang, S.; Ye, N. J. Am. Chem. Soc. 2011, 133, 11458-11461.
- (9) Ivanova, B.; Spiteller, M. Spectrochim. Acta, Part A 2010, 77, 849–855.
- (10) Hu, Z. G.; Yoshimura, M.; Mori, Y.; Sasaki, T. J. Cryst. Growth **2005**, 275, 232–239.
- (11) Becker, P. Adv. Mater. 1998, 10, 979-992.
- (12) Chen, C. T.; Wu, B.; Jiang, A.; You, G. Sci. Sin., Ser. B 1985, 28, 235–243.
- (13) Chen, C. T.; Wu, Y.; Jiang, A.; Wu, B.; You, G. M.; Li, K. R.; Lin, S. J. J. Opt. Soc. Am. B 1989, 6, 616-621.
- (14) Chen, C. T.; Ye, N.; Lin, J.; Jiang, J.; Zeng, W.; Wu, B. Adv. Mater. 1999, 11, 1071–1078.
- (15) Lei, S.; Huang, Q.; Zheng, Y.; Jiang, A.; Chen, C. T. Acta Crystallogr., Sect. C: Cryst. Struct. Commun. 1989, 45, 1861–1863.
- (16) Zhao, S.; Gong, P.; Bai, L.; Xu, X.; Zhang, S.; Sun, Z.; Lin, Z.; Hong, M.; Chen, C. T.; Luo, J. Nat. Commun. 2014, 5, 4019.
- (17) Zhao, S.; Kang, L.; Shen, Y.; Wang, X.; Asghar, M. A.; Lin, Z.; Xu, Y.; Zeng, S.; Hong, M.; Luo, J. *J. Am. Chem. Soc.* **2016**, *138*, 2961–
- (18) Huang, H. W.; Yao, J. Y.; Lin, Z. S.; Wang, X. Y.; He, R.; Yao, W. J.; Zhai, N. X.; Chen, C. T. Chem. Mater. 2011, 23, 5457–5463.
- (19) Zhao, S.; Gong, P.; Luo, S.; Liu, S.; Li, L.; Asghar, M. A.; Khan, T.; Hong, M.; Lin, Z.; Luo, J. *J. Am. Chem. Soc.* **2015**, *137*, 2207–2210.
- (20) Yang, G.; Peng, G.; Ye, N.; Wang, J.; Luo, M.; Yan, T.; Zhou, Y. Chem. Mater. 2015, 27, 7520–7530.
- (21) Zou, G.; Huang, L.; Ye, N.; Lin, C.; Cheng, W.; Huang, H. J. Am. Chem. Soc. 2013, 135, 18560–18566.
- (22) Jiang, X.; Luo, S.; Kang, L.; Gong, P.; Huang, H. W.; Wang, S.; Lin, Z.; Chen, C. T. ACS Photonics 2015, 2, 1183–1191.
- (23) Xia, M. J.; Li, R. K. J. Solid State Chem. 2013, 197, 366-369.
- (24) Yao, W.; Huang, H. W.; Yao, J.; Xu, T.; Jiang, X.; Lin, Z.; Chen, C. T. *Inorg. Chem.* **2013**, *52*, *6136–6141*.
- (25) Zhao, J.; Xia, M.; Li, R. K. J. Cryst. Growth 2011, 318, 971–973.
- (26) Wang, L.; Pan, S.; Chang, L.; Hu, J.; Yu, H. Inorg. Chem. 2012, 51, 1852-1858.
- (27) Zhao, S. G.; Zhang, G. C.; Yao, J. Y.; Wu, Y. C. CrystEngComm 2012, 14, 5209-5214.
- (28) Chang, H. Y.; Kim, S. H.; Halasyamani, P. S.; Ok, K. M. *J. Am. Chem. Soc.* **2009**, 131, 2426–2427.
- (29) Chang, H. Y.; Kim, S. H.; Ok, K. M.; Halasyamani, P. S. J. Am. Chem. Soc. **2009**, 131, 6865–6873.
- (30) Pan, S. L.; Smit, J. P.; Watkins, B.; Marvel, bM. R.; Stern, C. L.; Poeppelmeier, K. R. J. Am. Chem. Soc. 2006, 128, 11631–11634.
- (31) Nguyen, S. D.; Yeon, J.; Kim, S. H.; Halasyamani, P. S. *J. Am. Chem. Soc.* **2011**, 133, 12422–12425.
- (32) Chen, C. T. Sci. Sin. 1979, 22, 756.
- (33) Chen, C. T. In *Materials for Nonlinear Optics*; Marder, S. R., Sohn, J. E., Stucky, G. D., Eds.; ACS Sympsium Series; American Chemical Society: Washington, DC, 1991; Vol. 455, Chapter 24, pp 360–379.
- (34) Chen, C. T.; Bai, L.; Wang, Z. Z.; Li, R. K. J. Cryst. Growth 2006, 292, 169–178.
- (35) Wu, Y.; Sasaki, T.; Nakai, S.; Yokotani, A.; Tang, H.; Chen, C. T. Appl. Phys. Lett. 1993, 62, 2614–2615.
- (36) Mori, Y.; Kuroda, I.; Nakajima, S.; Sasaki, T.; Nakai, S. Appl. Phys. Lett. 1995, 67, 1818–1820.
- (37) Chemla, D. S.; Kupecek, P. J.; Robertson, D. S.; Smith, R. C. Opt. Commun. 1971, 3, 29–31.
- (38) Yu, H. W.; Wu, H. P.; Pan, S. L.; Yang, Z. H.; Su, X.; Zhang, F. F. J. Mater. Chem. **2012**, 22, 9665–9670.
- (39) Mei, L.; Wang, Y.; Chen, C. T.; Wu, B. J. Appl. Phys. 1993, 74,
- (40) Zou, G. H.; Ye, N.; Huang, L.; Lin, X. S. J. Am. Chem. Soc. 2011, 133, 20001–20007.

(41) Huang, H. W.; Yao, J. Y.; Lin, Z. S.; Wang, X. Y.; He, R.; Yao, W. J.; Zhai, N. X.; Chen, C. T. Angew. Chem., Int. Ed. 2011, 50, 9141.

- (42) Lee, M.-H.; Yang, C.-H.; Jan, J.-H. Phys. Rev. B: Condens. Matter Mater. Phys. 2004, 70, 235110.
- (43) Lo, C.-h. Master Degree Thesis, Tamkang University, New Taipei, Taiwan, 2005.
- (44) McMillen, C. D.; Stritzinger, J. T.; Kolis, J. W. Inorg. Chem. **2012**, *51*, 3953–3955.
- (45) Huang, Z.; Su, X.; Pan, S. L.; Dong, X.; Han, S.; Yu, H.; Zhang, M.; Yang, Y.; Cui, S.; Yang, Z. H. Scr. Mater. 2013, 69, 449–452.
- (46) Wu, H. P.; Yu, H. W.; Yang, Z. H.; Hou, X.; Su, X.; Pan, S. L.; Poeppelmeier, K. R.; Rondinelli, J. M. J. Am. Chem. Soc. 2013, 135, 4215–4218.
- (47) Zhang, F.; Jing, Q.; Zhang, F.; Pan, S. L.; Yang, Z.; Han, J.; Zhang, M.; Han, S. J. Mater. Chem. C 2014, 2, 667–674.
- (48) Clark, S. J.; Segall, M. D.; Pickard, C. J.; Hasnip, P. J.; Probert, M. J.; Refson, K.; Payne, M. C. Z. Kristallogr. Cryst. Mater. **2005**, 220, 567–570.
- (49) Pfrommer, B. G.; Cote, M.; Louie, S. G.; Cohen, M. L. J. Comput. Phys. 1997, 131, 233-240.
- (50) Perdew, J. P.; Burke, K.; Ernzerhof, M. Phys. Rev. Lett. 1996, 77, 3865–3868.
- (51) Lee, M.-H. Ph.D. Thesis; The University of Cambridge, Cambridge, U.K., 1996.
- (52) Lin, J. S.; Qteish, A.; Payne, M.; Heine, V. Phys. Rev. B: Condens. Matter Mater. Phys. 1993, 47, 4174-4180.
- (53) Rappe, A. M.; Rabe, K. M.; Kaxiras, E.; Joannopoulos, J. D. Phys. Rev. B: Condens. Matter Mater. Phys. 1990, 41, 1227–1230.
- (54) Aversa, C.; Sipe, J. E. Phys. Rev. B: Condens. Matter Mater. Phys. 1995, 52, 14636–14645.
- (55) Lin, J.; Lee, M.-H.; Liu, Z. P.; Chen, C. T.; Pickard, C. J. Phys. Rev. B: Condens. Matter Mater. Phys. 1999, 60, 13380-13389.
- (56) Zhang, B.; Lee, M.-H.; Yang, Z. H.; Jing, Q.; Pan, S. L.; Zhang, M.; Wu, H. P.; Su, X.; Li, C. S. Appl. Phys. Lett. **2015**, 106, 031906–031911.
- (57) Zhang, B.; Yang, Z.; Yang, Y.; Lee, M.-H.; Pan, S. L.; Jing, Q.; Su, X. J. Mater. Chem. C 2014, 2, 4133–4141.
- (58) Su, X.; Wang, Y.; Yang, Z.; Huang, X.-C.; Pan, S. L.; Li, F.; Lee, M.-H. J. Phys. Chem. C 2013, 117, 14149-14157.
- (59) Zou, G.; Zhang, L.; Ye, N. CrystEngComm 2013, 15, 2422–2427.
- (60) Chen, G.; Wu, Y.; Fu, P. J. Cryst. Growth 2006, 292, 449-453.
- (61) Wang, Y.; Pan, S. L. Coord. Chem. Rev. 2015, DOI: 10.1016/j.ccr.2015.12.008.
- (62) Heyward, C.; McMillen, C.; Kolis, J. Inorg. Chem. 2012, 51, 3956–3962.
- (63) He, R.; Lin, Z. S.; Zheng, T.; Huang, H.; Chen, C. T. J. Phys.: Condens. Matter 2012, 24, 145503-6pp.
- (64) Yao, W. J.; He, R.; Wang, X. Y.; Lin, Z. S.; Chen, C. T. Adv. Opt. Mater. 2014, 2, 411–417.
- (65) Cohen, A. J.; Mori-Sánchez, P.; Yang, W. Phys. Rev. B: Condens. Matter Mater. Phys. 2008, 77, 115123.
- (66) Mori-Sánchez, P. M.; Cohen, A. J.; Yang, W. Phys. Rev. Lett. 2008, 100, 146401.
- (67) Perdew, J. P.; Levy, M. Phys. Rev. Lett. 1983, 51, 1884–1887.
- (68) Godby, R. W.; Schluter, M.; Sham, L. J. Phys. Rev. B: Condens. Matter Mater. Phys. 1988, 37, 10159-10175.
- (69) Hybertsen, M. S.; Louie, S. G. Phys. Rev. B: Condens. Matter Mater. Phys. 1986, 34, 5390-5413.
- (70) Wang, C. S.; Klein, B. M. Phys. Rev. B: Condens. Matter Mater. Phys. 1981, 24, 3417–3429.